

## Article

# Distinctions of the Emergence of Convective Flows at the “Diffusion–Convections” Boundary in Isothermal Ternary Gas Mixtures with Carbon Dioxide

Vladimir Kossov <sup>1,\*</sup> , Dauren Zhakebayev <sup>2</sup> , Olga Fedorenko <sup>3,\*</sup>  and Ainur Zhumali <sup>2</sup> 

<sup>1</sup> Department of Physics, Institute of Mathematics, Physics and Informatics, Abai Kazakh National Pedagogical University, 13 Dostyk Ave., Almaty 050010, Kazakhstan

<sup>2</sup> Faculty of Mechanics and Mathematics, Al-Farabi Kazakh National University, 71 Al-Farabi Ave., Almaty 050040, Kazakhstan; dauren.zhakebayev@gmail.com (D.Z.); ainura.z89@gmail.com (A.Z.)

<sup>3</sup> Institute of Experimental and Theoretical Physics, Al-Farabi Kazakh National University, 71 Al-Farabi Ave., Almaty 050040, Kazakhstan

\* Correspondence: kosov\_vlad\_nik@list.ru (V.K.); fedor23.04@mail.ru (O.F.); Tel.: +7-7771606156 (V.K.)

**Abstract:** This study discusses the influence of the composition of a ternary gas mixture on the possibility of occurrence of convective instability under isothermal conditions due to the difference in the diffusion abilities of the components. A numerical study was carried out to study the change in “diffusion–concentration gravitational convection” modes in an isothermal three-component gas mixture He + CO<sub>2</sub> – N<sub>2</sub>. The mixing process in the system under study was modeled at different initial carbon dioxide contents. To carry out a numerical experiment, a mathematical algorithm based on the D2Q9 model of lattice Boltzmann equations was used for modeling the flow of gases. We show that the model presented in the paper allows one to study the occurrence of convective structures at different heavy component contents (carbon dioxide). It has been established that in the system under study, the instability of the mechanical equilibrium occurs when the content of carbon dioxide in the mixture is more than 0.3 mole fractions. The characteristic times for the onset of convective instability and the subsequent creation of structural formations, the values of which depend on the initial content of carbon dioxide in the mixture, have been determined. Distributions of concentration, pressure and kinetic energy that allow one to specify the types of mixing and explain the occurrence of convection for a situation where, at the initial moment of time, the density of the gas mixture in the upper part of the diffusion channel is less than in the lower one, were obtained.

**Keywords:** convection; diffusion; instability of mechanical equilibrium; ternary gaseous mixtures; isoconcentration lines; lattice Boltzmann method; D2Q9 model



**Citation:** Kossov, V.; Zhakebayev, D.; Fedorenko, O.; Zhumali, A. Distinctions of the Emergence of Convective Flows at the “Diffusion–Convections” Boundary in Isothermal Ternary Gas Mixtures with Carbon Dioxide. *Fluids* **2024**, *9*, 47. <https://doi.org/10.3390/fluids9020047>

Academic Editors: Jie Bao and Leonardo Santos de Brito Alves

Received: 29 October 2023

Revised: 22 January 2024

Accepted: 8 February 2024

Published: 12 February 2024



**Copyright:** © 2024 by the authors. Licensee MDPI, Basel, Switzerland. This article is an open access article distributed under the terms and conditions of the Creative Commons Attribution (CC BY) license (<https://creativecommons.org/licenses/by/4.0/>).

## 1. Introduction

Modern production technologies of various materials, forecasting natural phenomena, require an adequate description of the processes of heat and mass transfer in liquid and gaseous media, which, as a rule, are mixtures of various substances with a large number of components [1,2]. Difficulties in describing multicomponent mixtures are determined by the presence of several mechanisms of heat and mass transfer (convection, thermal conductivity, diffusion, thermal diffusion, diffusion thermal conductivity) and the need to take into account cross effects [3]. To control the behavior of such systems, new knowledge of the features of combined mass transfer is required, not only in the diffusion or in convective stages of mixing but also at the boundary of the kinetic transition between these regimes. In this case, the occurrence of convective flows is associated with the instability of the mechanical equilibrium of a multicomponent system and has some characteristic features that require more detailed study.

The results on the study of the stability of binary mixtures in a nonuniform temperature field in vertical cavities were generalized in monographs [4,5] and showed that monotonic

and oscillatory instabilities can arise in such systems. In these works, it was noted that the generation of a convective flow in a gravity field is associated not only with the distribution of the density of the studied mixture in a channel of a given geometry but also with the thermo-concentration characteristics of the mixture. With an initially unstable density stratification of the system, which assumes the condition when a heavier medium is above a light liquid (or gas), Rayleigh–Taylor convection is realized [6]. Various features of thermal concentration mixing associated with boundary conditions, interfaces between components, the occurrence of combined flows, described in numerous theoretical and experimental articles, are traditionally summarized in specialized reviews similar to [7] and allow one to follow the current trends in the development of this problem. With the opposite direction of the mixture density gradient, the occurrence of oscillatory instability is associated with the diverse effects of temperature and concentration gradients [8–11]. Research in the field of stability analysis of non-isothermal systems containing three or more components, in which the density of the mixture decreases with height, is much less abundant. In terms of calculation and theory, it was shown that the extension of the approach [4,5] to the study of the stability of the equilibrium of a system, a stationary flow in a vertical layer at different temperatures at the boundaries, has a complex structure [12,13]. In particular, attention is drawn to the existence of several regions of instabilities. This approach made it possible in [14,15] to investigate the occurrence of convection in cavities of various geometries at steady temperature and concentration gradients. A common feature of the studies carried out in [4,5,12–15] was the fixation of the destabilizing effect of temperature (heating from below) at low concentration gradients, which does not allow one to detail the role of the difference in the diffusion coefficients of the components in the formation of density inversion [16], which causes gravitational convection for the limiting isothermal case of multicomponent mixing.

Experimental and computational–theoretical studies for isothermal multicomponent mixing have shown that in gas mixtures, when the condition of decreasing density with height is realized, convective flows that are not typical for diffusion mixing may occur [17–21]. The difference in the diffusion activity of the components causes a violation of the stability of the system and the appearance of isothermal concentration gravitational convection with a synergistic increase in the rate of mixing of the components. The intensity of mixing in this case depends non-linearly on the ratios between the diffusion coefficients, pressure and a number of other thermophysical characteristics. It was shown that the presence of a stable resulting stratification in a gas mixture is not a guarantee of the absolute stability of the mechanical equilibrium of the system, since the components have different diffusion rates. This seemingly paradoxical nature of the emerging movement is explained by the unstable stratification of at least one of the components in the system. Due to the different diffusion coefficients, spatial redistribution of dissolved substances in the gravity field occurs, followed by the release of the potential energy of the component with the highest molecular weight, which is converted into the energy of the moving medium. The technique [17–21] was recommended for determining the spectrum of thermophysical and geometric parameters, at which the transition from the diffusion state to the convective one occurs, assessing the role of diffusion mechanisms that form inversion layers, leading to the emergence of gravitational convection, which was presented in [22,23] for special cases of multicomponent mixing. However, the stability analysis formalism used in [22,23] does not allow one to monitor the emergence of structural formations and the subsequent evolution of convective flows. The solution of such issues related to the study and refinement of separation mechanisms in isothermal multicomponent gas mixtures seems important for the problems of combined mass transfer and requires further consideration.

The aim of this work is to numerically study the change in “diffusion–concentration gravitational convection” modes in an isothermal three-component gas mixture, in which the diffusion coefficients of the components differ significantly from each other. A ternary mixture of helium, carbon dioxide and nitrogen is considered for various initial compositions for a situation in which the density of the mixture decreases with height. Mixing

occurs at room temperature and elevated pressures. The choice of the proposed system is also due to the fact that some features of combined mass transfer in a given mixture were studied experimentally [23], which will allow for validation with the obtained calculations. Numerical studies in model situations will make it possible to recommend the composition of mixtures, pressure and temperature, under which it is possible to achieve the mode of preferential transfer of a component with given thermophysical properties, which seems to be relevant for systems containing greenhouse gases. This study presents a calculation to determine the boundary of the “diffusion–concentration gravitational convection” regime change. The distributions of concentration, pressure and average kinetic energy in a vertical cylindrical channel are analyzed. The obtained results of the numerical study are compared with experimental data.

The presented article is divided into the following sections. Section 2 presents the mathematical formulation of the problem, the basic equations and the numerical method for solving them. Section 3 presents the distributions of concentration, pressure and average kinetic energy in the computational domain. Section 4 completes the paper and includes the main conclusions.

## 2. Mathematical Formulation of the Problem and Numerical Methods

The description of convective flows caused by the instability of the mechanical equilibrium in the system is based on the solution of the general system of hydrodynamic equations, which includes the Navier–Stokes equations, the conservation of the number of mixture particles and components, as well as the corresponding initial and boundary conditions. Various numerical approaches [24–31] are used to solve this system of equations. For this study, the application of one or another approach depends on the ability to describe the emerging types of flows that are realized as a result of the instability of mechanical equilibrium during diffusion. For example, for the case of a binary isothermal mixture, the results of numerical simulation of convective flows in an inclined channel based on the lattice Boltzmann equations method (LBM) were presented in [27]. The validation of the numerical solver is presented in [31], where the numerical solutions are compared with the analytical solutions of the plane channel flow and are found to be in good agreement. Verification of the numerical results in the framework of the proposed calculation scheme with experimental data showed satisfactory agreement. Therefore, in this paper, the method tested for binary systems is extended to the case of isothermal ternary gas mixtures. In this case, both the possibility of the emergence of a convective mixing mechanism and the dynamics of the process are considered.

Consider a mixing process in a cylindrical channel in which a mixture of two components is mixed with a third gas. The problem statement is illustrated in Figure 1. The upper part of channel  $S_1$  contains gas 1 (with the minimum molar mass  $M_1$ ) and gas 2 (which has the highest molecular weight  $M_2$ ) diffusing into gas 3 (with an intermediate molar mass  $M_3$ ) located in the lower part of channel  $S_2$ . The condition  $M_2 > M_3 > M_1$  is satisfied for the molecular weights of the components. We consider a two-dimensional region of the cross-section of the cylindrical region  $H \times d$  in the Cartesian coordinate system (Figure 1a).

The change in “diffusion–convection” modes in ternary gas mixtures is described by the system of Navier–Stokes hydrodynamic equations. Taking into account the condition of independent diffusion, for an isothermal gas mixture  $\sum_{i=1}^3 j_i = 0$ , and  $\sum_{i=1}^3 c_i = 1$ , this system of equations can be written as [4,22,23]:

$$\begin{aligned} \rho \left[ \frac{\partial \vec{u}}{\partial t} + (\vec{u} \nabla \vec{u}) \right] &= -\nabla p + \eta \nabla^2 \vec{u} + \left( \frac{\eta}{3} + \zeta \right) \nabla \operatorname{div} \vec{u} + \rho \vec{g}, \\ \frac{\partial \rho_N}{\partial t} &= -\operatorname{div}(\rho_N \vec{v}), \\ \frac{\partial c_1}{\partial t} + \vec{v} \nabla c_1 &= \operatorname{div}[D_{11}^* \nabla c_1 + D_{12}^* \nabla c_2], \\ \frac{\partial c_2}{\partial t} + \vec{v} \nabla c_2 &= \operatorname{div}[D_{21}^* \nabla c_1 + D_{22}^* \nabla c_2], \end{aligned} \tag{1}$$

where  $\vec{u}$  is the mass-average velocity,  $\vec{v}$  is the number-average velocity of the ternary mixture,  $\rho$  is the density,  $p$  is the pressure,  $\eta$  and  $\xi$  are the coefficients of shear and bulk viscosity,  $\vec{g}$  is the gravity acceleration vector,  $\rho_N$  is the number density,  $t$  is the time,  $c_i$  is the concentration of the  $i$ th component,  $\vec{j}_i$  is the density of the diffusion flux of the  $i$ -th component and  $D_{ij}^*$  is the practical diffusion coefficients.

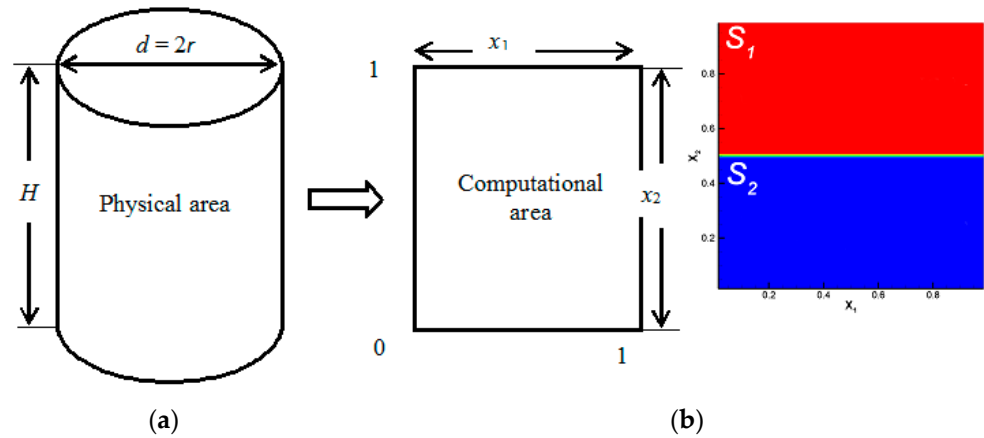


**Figure 1.** Simulation of mass transfer at the boundary of regime change: (a) physical and calculated mixing areas; (b) initial conditions for placing ternary mixtures in a diffusion channel.

The equation of medium state is written in the traditional form:

$$\rho = \rho(c_1, c_2, p), T = \text{const.} \tag{2}$$

The system of Equations (1) and (2) characterizes a wide class of motions in gas mixtures, including descriptions of concentration gravitational convection (or convective instability), which is determined by the existence in the gravity field of spatial density inhomogeneity caused by the nonuniformity of the concentration of components. At the same time, there are a number of studies of convection under conditions where the compressibility of the medium is insignificant [4,5,10]. In this case, simplifications in the system (1)–(2) suppose that density inhomogeneities caused by compositional nonuniformities are assumed to be small and are taken into account only in the lift term in the Navier–Stokes equation of motion. In this case, the lift force is determined by a value that is calculated within the framework of the Boussinesq approximation [4,5]:

$$\rho g = \rho_0 g (1 - \beta_1 c_1' - \beta_2 c_2'), \tag{3}$$

where  $c_i'$  is the concentration perturbation of the  $i$ -th component relative to the average value  $\langle c_i \rangle$  taken as the reference point ( $\langle c_i \rangle \gg c_i'$ ),  $\beta_i = \frac{1}{\rho_0} \left( \frac{\partial \rho}{\partial c_i} \right)_{p, T, c_j}$ ;  $\rho_0$  is the average value of mixture density.

Solving the system of Equations (1)–(3) by the method of small perturbations, one can obtain the equations of concentration convection for the perturbed quantities (primes are omitted):

$$\begin{aligned} \frac{\partial \vec{u}}{\partial t} + (\vec{u} \nabla) \vec{u} &= -\frac{1}{\rho_0} \nabla p + \nu \nabla^2 \vec{u} + g(\beta_1 c_1 + \beta_2 c_2) \vec{\gamma}, \\ \frac{\partial c_1}{\partial t} + \vec{v} \nabla \langle c_1 \rangle &= D_{11}^* \nabla^2 c_1 + D_{12}^* \nabla^2 c_2, \\ \frac{\partial c_2}{\partial t} + \vec{v} \nabla \langle c_2 \rangle &= D_{21}^* \nabla^2 c_1 + D_{22}^* \nabla^2 c_2, \\ \text{div} \vec{v} &= 0, \end{aligned} \tag{4}$$

where  $\vec{\gamma}$  is the unit vector and  $\nu$  is the kinematic viscosity coefficient.

Differences in perturbations of the mass-average and number-average velocities are of the same order. Therefore, when  $H \gg r$  (where  $H$  is the height of the diffusion channel,  $r$  is the radius of the diffusion channel),  $\vec{v}$  can be replaced by  $\vec{u}$  [22,23].

The boundary conditions are specified as follows:

$$\vec{u}(\vec{x}, t) = 0, \frac{\partial c_i}{\partial \vec{n}} = 0, i = 1 - 3,$$

where  $\vec{n} = (n_1, n_2)$  is the outer normal to the boundary of the computational domain.

Dirichlet boundary conditions are set at the upper and lower boundaries for pressure:  $p = 0$ . Neumann conditions are specified on the lateral boundaries:  $\frac{\partial p}{\partial x} = 0$ .

The initial conditions are written as follows:

$$\begin{aligned} \vec{u}(\vec{x}, t = 0) &= 0, \\ c_1(\vec{x}, t = 0) \Big|_{\vec{x} \in S_1} &= X_1, c_1(\vec{x}, t = 0) \Big|_{\vec{x} \in S_2} = 0, \\ c_2(\vec{x}, t = 0) \Big|_{\vec{x} \in S_1} &= X_2, c_2(\vec{x}, t = 0) \Big|_{\vec{x} \in S_2} = 0, \\ c_3(\vec{x}, t = 0) \Big|_{\vec{x} \in S_1} &= 0, c_3(\vec{x}, t = 0) \Big|_{\vec{x} \in S_2} = X_3, \end{aligned}$$

where  $X_i$  is the concentrations of components in the upper  $S_1$  and lower  $S_2$  regions.

To establish a connection between the parameters and conditions of the process, which allows one to comprehensively analyze a large number of geometric and thermophysical characteristics, we transition to a dimensionless formulation of the problem (1)–(4). Let us introduce the following scales of units:  $H$  is the characteristic linear size of the cavity,  $H^2/\nu$  is the time,  $D_{22}^*/H$  is the velocity,  $A_i H$  is the concentrations of the  $i$ -th component and  $\rho_0 \nu D_{22}^*/H^2$  is the pressure. The system of Equation (4) in dimensionless quantities is transformed into the following equations:

$$\begin{aligned} \frac{\partial \vec{u}}{\partial t} + \frac{1}{Pr_{22}} \nabla (\vec{u} \cdot \vec{u}) &= -\nabla p + \Delta \vec{u} + (Ra_1 d_{11} c_1 + Ra_2 c_2) \vec{\gamma}, \\ \frac{\partial c_1}{\partial t} + \frac{1}{Pr_{22}} \vec{u} \nabla c_1 &= \frac{1}{Pr_{11}} \Delta c_1 + q_1, \\ \frac{\partial c_2}{\partial t} + \frac{1}{Pr_{22}} \vec{u} \nabla c_2 &= q_2 + \frac{1}{Pr_{22}} \Delta c_2, \\ \text{div } \vec{u} &= 0, \end{aligned} \tag{5}$$

where  $Pr_{ii} = \nu/D_{ii}^*$  is the Prandtl diffusion number, and  $Ra_i = g\beta_i A_i H^4/D_{ii}^* \nu$  is the partial Rayleigh number. These numbers serve as the similarity criteria for the free convective movement. Values  $d_{ij} = D_{ij}^*/D_{22}^*$  are the parameters that determine the relationship between practical diffusion coefficients,  $q_1 = \frac{1}{Pr_{22}} d_{12} \Delta c_2$  and  $q_2 = \frac{A_1}{A_2} \frac{1}{Pr_{22}} d_{21} \Delta c_1$  on the right side of the equations for the concentration of components considered as sources, where  $A_i$  is the dimensionless initial concentration gradient of the  $i$ -th component.

The dimensionless boundary conditions are given as follows:

$$\begin{aligned} \vec{u}(\vec{x}, t) &= 0, \frac{\partial c_i}{\partial \vec{n}} = 0, i = 1 - 3, \\ p \Big|_{x_2 = 0} &= 0, \frac{\partial p}{\partial x} \Big|_{x_1 = 0} = 0, \\ x_2 &= 1, x_1 &= 1 \end{aligned}$$

The dimensionless initial conditions are written as follows:

$$\begin{aligned} \vec{u}(\vec{x}, t = 0) &= 0, \\ c_1(\vec{x}, t = 0) \Big|_{\vec{x} \in S_1} &= 1, \quad c_1(\vec{x}, t = 0) \Big|_{\vec{x} \in S_2} = 0, \\ c_2(\vec{x}, t = 0) \Big|_{\vec{x} \in S_1} &= 1, \quad c_2(\vec{x}, t = 0) \Big|_{\vec{x} \in S_2} = 0, \\ c_3(\vec{x}, t = 0) \Big|_{\vec{x} \in S_1} &= 0, \quad c_3(\vec{x}, t = 0) \Big|_{\vec{x} \in S_2} = 1. \end{aligned}$$

The implementation of the developed mathematical model is based on the application of the D2Q9 scheme of the method of lattice Boltzmann equations [32], according to which the Boltzmann equation discretized in the space of velocities is solved. Discretization is carried out by replacing the continuous velocity of the particle with a discrete set of velocities. In the Bhatnagar–Gross–Krook (BGK) approximation, the lattice Boltzmann equation is written as follows:

$$\begin{aligned} f_i(\vec{x} + \vec{e}_i \Delta t, t + \Delta t) - f_i(\vec{x}, t) &= \Delta t \left[ -\frac{f_i(\vec{x}, t) - f_i^{eq}(\vec{x}, t)}{\tau_f} + F_i \right], \\ h_{i,\alpha}(\vec{x} + \vec{e}_i \Delta t, t + \Delta t) - h_{i,\alpha}(\vec{x}, t) &= \Delta t \left[ -\frac{h_{i,\alpha}(\vec{x}, t) - h_{i,\alpha}^{eq}(\vec{x}, t)}{\tau_{h,\alpha}} + Q_{i,\alpha} \right], \end{aligned} \tag{6}$$

where  $\alpha$  denotes the concentration component index,  $i$  is the direction of lattice velocity,  $f_i, h_{i,\alpha}$  are the velocity and concentration distribution functions of the  $\alpha$ -component,  $\vec{e}_i$  is the discrete lattice velocity in the  $i$  direction,  $\tau_f, \tau_{h,\alpha}$  are the relaxation times,  $F_i$  is the external force component,  $Q_{i,\alpha}$  is responsible for the source  $q_\alpha$ ,  $\Delta t$  is the lattice time step, and  $f_i^{eq}, h_{i,\alpha}^{eq}$  are the equilibrium distribution function of the velocity and concentration of the  $\alpha$ -component, respectively.

It is important to emphasize that the choice of numerical method depends on the specific context of the problem and the requirements for modeling accuracy. The BGK scheme for lattice Boltzmann equations can be used to analyze flows in microchannels and slow flows of liquids or low-velocity gases, where inertial effects are negligible compared to viscous effects. The BGK model approximates the collision operator by assuming a uniform relaxation time, which leads to a linearized interparticle interaction term. In this case, there is a trade-off between modeling accuracy and computational efficiency. Calculations for large relaxation times were not carried out.

For equilibrium functions, it is valid:

$$\begin{aligned} f_i^{eq} &= \omega_i \rho \left[ 1 + 3 \frac{\vec{e}_i \vec{u}}{c^2} + \frac{9}{2} \frac{(\vec{e}_i \vec{u})^2}{c^4} - \frac{3}{2} \frac{\vec{u} \vec{u}}{c^2} \right], \\ h_{i,\alpha}^{eq} &= \omega_i C_\alpha \left[ 1 + 3 \frac{\vec{e}_i \vec{u}}{c^2} + \frac{9}{2} \frac{(\vec{e}_i \vec{u})^2}{c^4} - \frac{3}{2} \frac{\vec{u} \vec{u}}{c^2} \right], \end{aligned} \tag{7}$$

where  $c = \Delta x / \Delta t$ , and  $\Delta x$  and  $\Delta t$  are the lattice step in space and time, respectively, which are equal to one. The weight coefficients  $\omega_i$  in the directions  $i$ , which are included in the expressions for the equilibrium functions (7), have the following values:

$$\omega_i = \begin{cases} 4/9, & i = 0, \\ 1/9, & i = 1, 2, 3, 4, \\ 1/36, & i = 5, 6, 7, 8. \end{cases}$$

For the D2Q9 model, the interpretation of which is shown in Figure 2, it is characteristic that the discrete velocities are given by the expressions:

$$\begin{aligned} e_0 &= (0, 0), e_1 = (1, 0), e_2 = (0, 1), e_3 = (-1, 0), e_4 = (0, -1), \\ e_5 &= (1, 1), e_6 = (-1, 1), e_7 = (-1, -1), e_8 = (1, -1). \end{aligned}$$

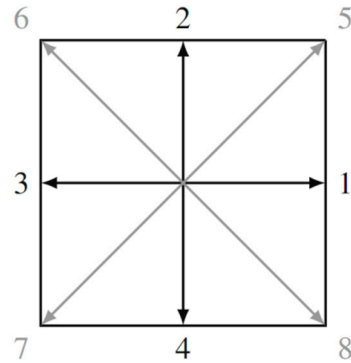


Figure 2. Two-dimensional lattice D2Q9 with nine discrete velocities.

To approximate the external force  $\vec{F} = \rho_r g [\beta_{C_1} (C_1 - C_r) + \beta_{C_2} (C_2 - C_r)]$  in LBM, the scheme proposed by Guo et al. [33] is used:

$$F_i = \omega_i \left( 1 - \frac{\Delta t}{2\tau_f} \right) \left[ \frac{\vec{e}_i - \vec{u}}{c_s^2} + \frac{\vec{e}_i (\vec{e}_i \cdot \vec{u})}{c_s^4} \right] \cdot \vec{F}.$$

In accordance with the development of Seta [34], the sources of  $q_\alpha$  are approximated using the following formula:

$$Q_{i,\alpha} = \omega_i \left( 1 - \frac{1}{2\tau_{h,\alpha}} \right) q_\alpha.$$

The evolution equation is divided into two stages: first, the collision is taken into account (1), and then the propagation is taken into consideration (2):

$$\begin{aligned} 1. \quad \tilde{f}_i(\vec{x}, t) &= f_i(\vec{x}, t) + \Delta t \left( -\frac{f_i(\vec{x}, t) - f_i^{eq}(\vec{x}, t)}{\tau_f} + F_i \right), \\ \tilde{h}_{i,\alpha}(\vec{x}, t) &= h_{i,\alpha}(\vec{x}, t) + \Delta t \left( -\frac{h_{i,\alpha}(\vec{x}, t) - h_{i,\alpha}^{eq}(\vec{x}, t)}{\tau_{h,\alpha}} + Q_{i,\alpha} \right), \\ 2. \quad \bar{f}_i(\vec{x} + \vec{e}_i \Delta t, t + \Delta t) &= \tilde{f}_i(\vec{x}, t), \\ \bar{h}_{i,\alpha}(\vec{x} + \vec{e}_i \Delta t, t + \Delta t) &= \tilde{h}_{i,\alpha}(\vec{x}, t). \end{aligned}$$

Further, corrections are made for macro parameters (density, velocity, concentration):

$$\rho = \sum_{i=0}^8 \bar{f}_i, \quad \rho \vec{u} = \sum_{i=0}^8 \bar{f}_i \vec{e}_i + \frac{\Delta t}{2} \vec{F}, \quad C_\alpha = \sum_{i=0}^8 \left( \bar{h}_{i,\alpha} + \frac{\Delta t}{2} Q_{i,\alpha} \right).$$

The system of equations is closed by the Dirichlet boundary conditions  $\bar{f}_i(\vec{x}_w, t + \Delta t) = \bar{f}_{-i}(\vec{x}_w, t + \Delta t)$ ,  $\vec{e}_i \cdot \vec{n} > 0$  for the velocity on all walls and the Neumann condition  $\bar{h}_{i,\alpha}(\vec{x}_w, t + \Delta t) = \bar{h}_{-i,\alpha}(\vec{x}_w, t + \Delta t)$ ,  $\vec{e}_i \cdot \vec{n} > 0$  for the concentration of components on all walls.

Simulations using the lattice Boltzmann equation are performed in lattice units, so it is necessary to relate all physical parameters to their lattice counterparts. This relationship is established by means of the unit conversion factor  $C_*$ .

It is recommended to set the lattice steps in position space equal to 1:  $\Delta x = 1, \Delta t = 1$ . Thus, the conversion coefficients for length and time will be equal to the dimensional values of the steps in physical units:  $C_H = \Delta x_{\text{phy}}, C_t = \Delta t_{\text{phy}}$ , where  $\Delta x_{\text{phy}}, \Delta t_{\text{phy}}$  represent physical steps through space and time. The index “phy” will denote physical quantities.

Based on the channel height and the node size, we determine the spatial step as  $\Delta x_{\text{phy}} = H/N$ . According to the stability conditions of LBM algorithms, the characteristic lattice velocity is  $u_{\text{lbm}} < 0.4$  for  $\tau \geq 0.55$ . In this work, the lattice velocity is set to  $u_{\text{lbm}} = 0.2$ . The conversion coefficient for velocity will be determined through  $C_u = u_{\text{phy}}/u_{\text{lbm}}$ , where the physical value of velocity is equal to  $u_{\text{phy}} = \sqrt{gH}$ . Then, the physical time step is equal to  $\Delta t_{\text{phy}} = \Delta x_{\text{phy}}/C_u$ .

Using the expression obtained as a result of the Chapman–Enskog analysis [32]  $\nu_f = c_s^2(\tau_f - 1/2)$  and the conversion factor for the kinematic viscosity  $C_\nu = C_H^2/C_t$ , we determine the lattice relaxation time as  $\tau_f = 3(\Delta t_{\text{phy}}/\Delta x_{\text{phy}}^2)\nu_f + 1/2$ .

In the same way, the analysis and determination of other model parameters are carried out.

### 3. Results of the Numerical Calculation

Numerical calculations were carried out on a uniform rectangular grid with a number of nodes of  $80 \times 80$  along the  $x_1, x_2$  axes, respectively. Calculations were performed for the physical parameters determined experimentally [35] or calculated from the kinetic concepts [36] for given geometric characteristics of the channel (see Table 1) and are shown in Figures 3–5. The length and height of the computational domain are  $L = 0.01$  m,  $H = 0.01$  m. Physical steps in space and time have the following values:  $\Delta x_{\text{phy}} = 0.000125$  and  $\Delta t_{\text{phy}} = 7.986 \cdot 10^{-5}$ .

**Table 1.** Some parameters of the mixture He (1) + CO<sub>2</sub> (2) – N<sub>2</sub> (3) at  $p = 0.101$  MPa,  $T = 298.0$  K [35,36].

Components	$\rho,$ kg/m <sup>3</sup>	$\eta,$ 10 <sup>−5</sup> Pa·s	$D_{12},$ 10 <sup>−4</sup> m <sup>2</sup> /s	$D_{13},$ 10 <sup>−4</sup> m <sup>2</sup> /s	$D_{23},$ 10 <sup>−4</sup> m <sup>2</sup> /s	Molar Mass, 10 <sup>−3</sup> kg/mole
He	0.160	1.977				4.003
CO <sub>2</sub>	1.841	1.463	0.61	0.71	0.165	44.011
N <sub>2</sub>	1.146	1.775				28.016

The correction factors for temperature and pressure required to find the experimental parameters will be denoted by  $K_t = T/T_0$  and  $K_p = p_0/p$ , respectively. Here,  $T_0 = 298.0$  K and  $p_0 = 0.1$  MPa, and  $T$  and  $p$  are the temperature and pressure of the experiment. The density and dynamic shear viscosity of the components at the experimental parameters are calculated using the formulas  $\rho_i = \rho_i^0/(K_p \times K_t)$  and  $\eta_i = \eta_i^0 K_t^{1/2}$ , where  $\rho_i^0$  is the density of the  $i$ -th component, and  $\eta_i^0$  is the dynamic viscosity of the  $i$ -th component corresponding to the conditions  $T_0 = 298.0$  K and  $p_0 = 0.1$  MPa. Kinematic viscosity is calculated using the formula  $\nu_f = \sum_i C_i \frac{\eta_i}{\rho_i}$ , where  $C_i$  is the concentration of the  $i$ -th component. The interdiffusion coefficients given in Table 1 at different pressures and temperatures are related to each other in the following way  $D_{ij} = D_{ij}^0 K_t^{3/2} K_p, i \neq j$ , where  $D_{ij}^0$  are the interdiffusion coefficients presented in Table 1. Practical diffusion coefficients  $D_{ij}^*$  and mutual diffusion coefficients are related to each other by the following relationships [22,23]:

$$D_{11}^* = \frac{D_{13}[C_1 D_{32} + (C_2 + C_3) D_{12}]}{D}, \quad D_{12}^* = -\frac{C_1 D_{23}(D_{12} - D_{13})}{D},$$

$$D_{22}^* = \frac{D_{23}[C_2 D_{13} + (C_1 + C_2) D_{12}]}{D}, \quad D_{21}^* = -\frac{C_2 D_{13}(D_{12} - D_{23})}{D},$$

$$D = C_1 D_{23} + C_2 D_{13} + C_3 D_{12}.$$



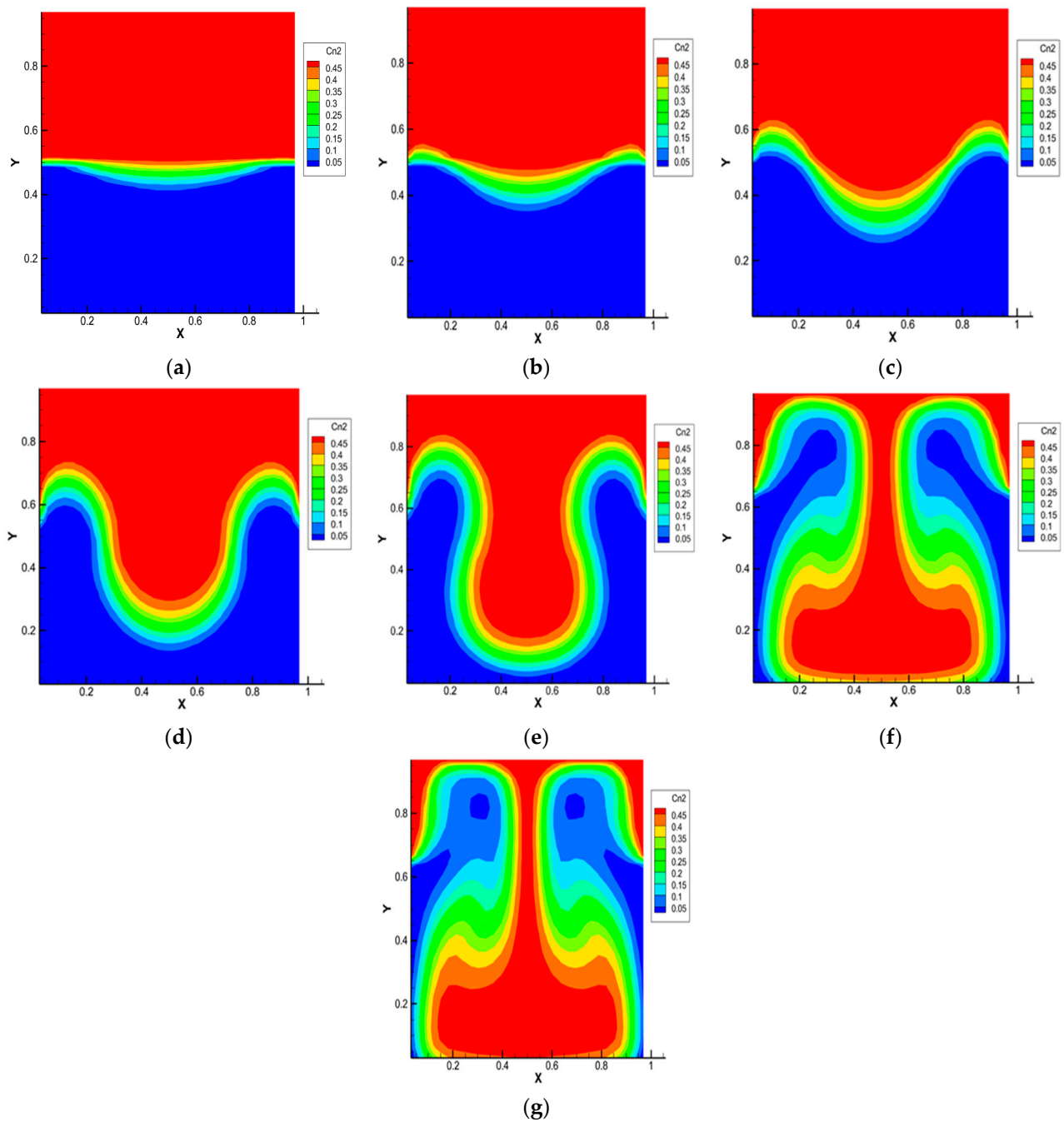


**Figure 3.** Carbon dioxide isoconcentration lines for the 0.5 He + 0.5 CO<sub>2</sub> – N<sub>2</sub> system, p = 1.0 MPa, T = 298.0 K, Ra<sub>1</sub> = 4.34, Ra<sub>2</sub> = 8.31. Characteristic mixing times: (a)—0.38 s; (b)—0.57 s; (c)—0.76 s; (d)—0.95 s; (e)—1.14 s; (f)—1.71 s; (g)—1.90 s.

The volumetric expansion coefficients for determining the partial Rayleigh numbers are found using the formulas:

$$\beta_{C_1} = \frac{m_1 - m_2}{H} (C_1 m_1 + C_2 m_2 + C_3 m_3), \quad \beta_{C_2} = \frac{m_2 - m_3}{H} (C_1 m_1 + C_2 m_2 + C_3 m_3),$$

where  $m_i$  is the molar mass of the  $i$ -th component.

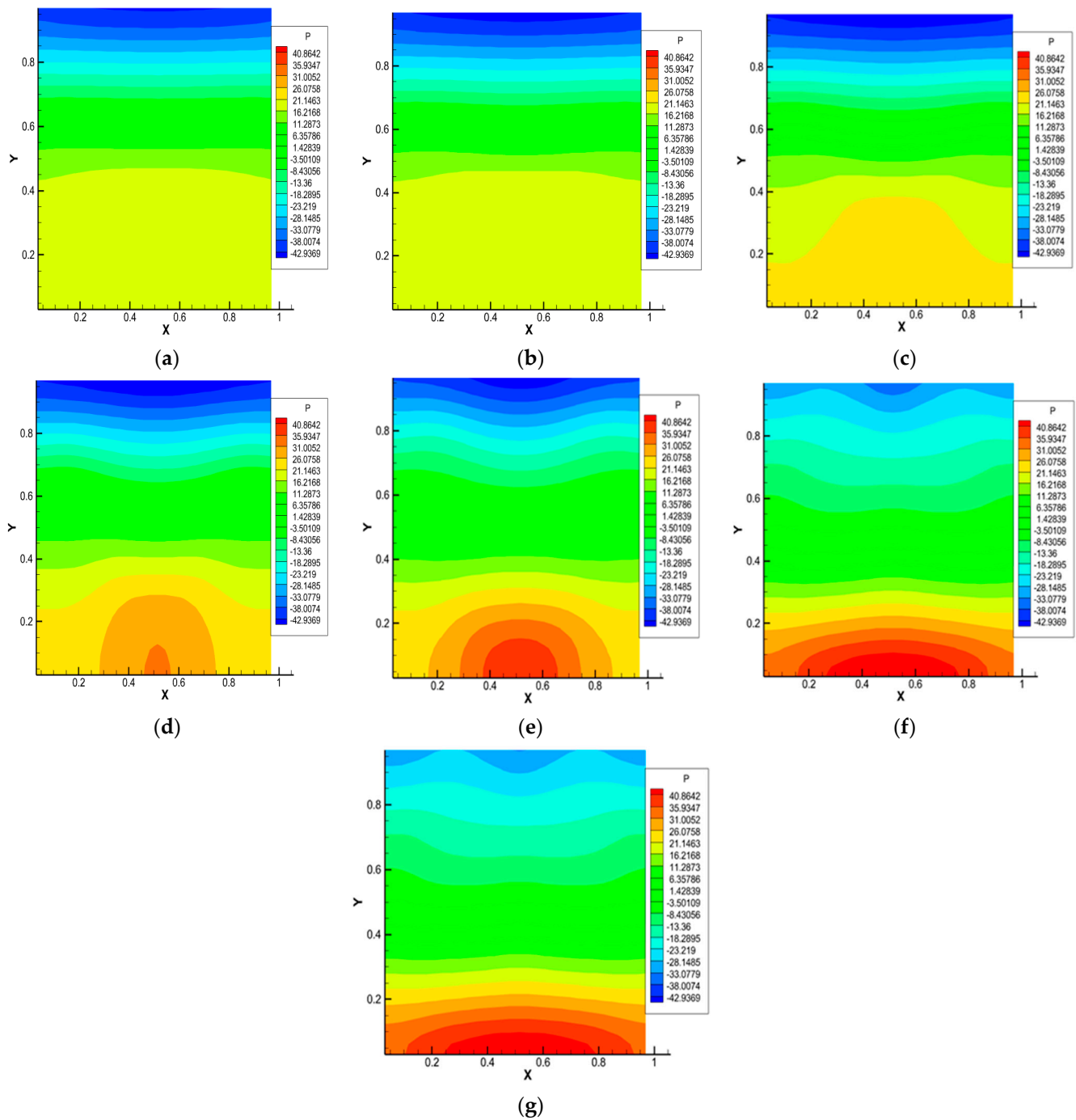


**Figure 4.** Pressure distribution for the 0.5 He + 0.5 CO<sub>2</sub> – N<sub>2</sub> system, p = 1.0 MPa, T = 298.0 K, Ra<sub>1</sub> = 4.34, Ra<sub>2</sub> = 8.31. Characteristic mixing times: (a)—0.38 s; (b)—0.57 s; (c)—0.76 s; (d)—0.95 s; (e)—1.14 s; (f)—1.71 s; (g)—1.90 s.

Figure 3 shows the isoconcentration lines of carbon dioxide at different mixing times of the ternary gas system 0.50 He (1) + 0.50 CO<sub>2</sub> (2) – N<sub>2</sub> (3) at pressure p = 1.0 MPa and T = 298.0 K. At t = 0 s, the density of the binary mixture located in the upper part of the diffusion channel is less than the density of nitrogen, which is localized in the lower part. Diffusion takes place at the initial stage (see Figure 3a). After 0.33 s, a violation of the monotonicity in the distribution of isoconcentration lines, which increases with time (Figure 3b,c), is recorded. Such a distribution is not characteristic of diffusion mixing. It can be assumed that, starting from this time, instability in the mechanical equilibrium, which is the cause of the appearance of convection, arises in the system under study. Figure 3d

shows the development of a convective cell, which begins 0.95 s after the start of mixing. At the final stage (Figure 3e–g), the convective formation begins to move in the gravity field relative to the diffusion interface. Then, but already under other initial condition, the process of structural formation begins again, but, already under other boundary conditions, i.e., in the system under study, the appearance of a drop convective mixing mode, which was recorded experimentally in various ternary mixtures [17,18,22], including those containing CO<sub>2</sub> [23], is possible.

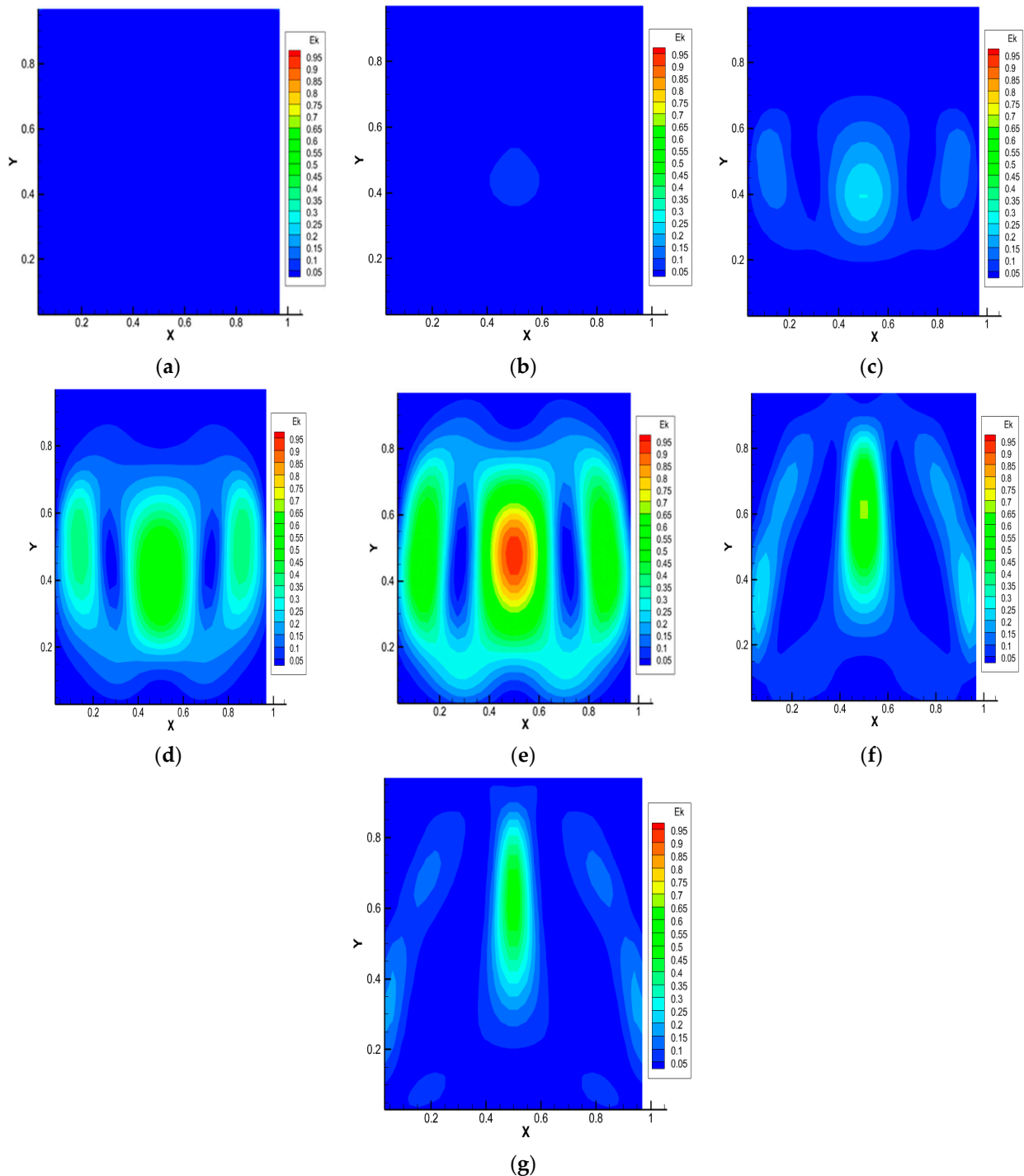


**Figure 5.** Average kinetic energy distribution for the 0.5 He + 0.5 CO<sub>2</sub> – N<sub>2</sub> system,  $p = 1.0$  MPa,  $T = 298.0$  K,  $Ra_1 = 4.34$ ,  $Ra_2 = 8.31$ . Characteristic mixing times: (a)—0.38 s; (b)—0.57 s; (c)—0.76 s; (d)—0.95 s; (e)—1.14 s; (f)—1.71 s; (g)—1.90 s.

The calculation results presented in Figure 3 are in qualitative agreement with the experimental data for the 0.44 He (1) + 0.56 CO<sub>2</sub> (2) – N<sub>2</sub> (3) system given in [22], which shows that at pressures above 0.5 MPa, the conditions for the preferential transfer of carbon dioxide are realized in the system. The main reason that does not allow for more accurate quantitative comparisons is the significant difference in the characteristic mixing time in the experimental diffusion cell (several thousand seconds) and the computational region (several seconds).

Figure 4 shows the pressure distributions under thermophysical conditions and characteristic mixing times corresponding to Figure 3. It is noteworthy that the largest pressure perturbations occur at times corresponding to the formation of a convective cell (Figure 4d,e). Further complex pressure fluctuations (Figure 4e–g) show the presence of zones of increased and decreased pressure in the system caused by the presence of complex convective formations.

Distributions of the average kinetic energy presented in Figure 5 show that its value is localized in certain coordinates of the model channel. This relates to the fact that convective flows arising due to the instability of mechanical equilibrium lead to a synergistic increase in the partial mixing of components. There is a change in the flow structure and mass transfer modes that are not typical for diffusion, which are sources of energy for the movement of convective formations in a closed system.

For cases where the content of carbon dioxide is more than 0.3 mole fractions in the system under consideration, the distributions of CO<sub>2</sub> concentrations, pressure and kinetic energy are similar to the distributions shown in Figures 3–5.

It should be assumed that the results of calculations on the distributions of concentrations, pressure and average kinetic energy shown in Figures 3–5 depend on the initial composition of the ternary mixture. From the analysis of Figure 3, we can suppose the existence of the following characteristic mixing modes: diffusion and the occurrence of mechanical equilibrium instability (Figure 3a–c), corresponding to times  $t_1$ – $t_3$ ; creation of structural convective formations (Figure 3d,e), which correspond to times  $t_4$  and  $t_5$ ; organization of the convective cell (Figure 3f,g) and its initial movement in the gravity field. It should be expected that the identified mixing stages are able to manifest themselves in a similar way with other initial compositions but with different characteristic times.

The partial Rayleigh numbers and mixing times ( $t_1$ – $t_7$ ) specifying diffusion, the onset and development of mechanical equilibrium instability, the occurrence of a structural formation and its subsequent evolution leading to an initial mixing in the channel due to the force gravity are listed in Table 2 for the various compositions of carbon dioxide in the ternary mixture of He + CO<sub>2</sub> – N<sub>2</sub>.

**Table 2.** Characteristic mixing times for the different compositions of carbon dioxide at  $p = 1.01$  MPa,  $T = 298.0$  K.

Molar Composition of CO <sub>2</sub> , mol. Fraction	Ra for CO <sub>2</sub>	$t_1$ , s	$t_2$ , s	$t_3$ , s	$t_4$ , s	$t_5$ , s	$t_6$ , s	$t_7$ , s
0.80	8.76	0.45	1.12	1.96	2.38	3.50	4.06	4.90
0.70	8.67	0.42	0.90	1.20	1.65	2.40	2.55	2.70
0.60	8.53	0.38	0.66	0.83	1.20	1.98	2.15	2.50
0.50	8.31	0.33	0.57	0.76	0.95	1.14	1.71	1.90
0.25	6.94	diffusion						

A weak dependence on the initial content of carbon dioxide in the mixture under study is observed at the time  $t_1$ , corresponding to the initial formation of the curvature of the isoconcentration lines. However, the difference in the characteristic mixing times  $t_2$  and  $t_3$  for different initial compositions becomes noticeable at subsequent stages of the development of mechanical equilibrium instability. The dependence on the concentration of CO<sub>2</sub> in the initial system becomes more significant at the stage of formation of convective cells with the corresponding times  $t_4$ ,  $t_5$  and the emergence of currents in

the initial development phase with mixing times  $t_6$ ,  $t_7$ . The identified trend shows that with an increase in the concentration of carbon dioxide in the initial mixture, more time is required for the development of mechanical equilibrium instability and the formation of convective structures. This can be explained by the fact that at high  $\text{CO}_2$  contents in the initial mixture, the partial helium flux, due to its small size, does not create conditions for the diffusion mechanisms that form the inversion density layers. In this case, the emergence of gravitational convection is carried out in the traditional way [6].

#### 4. Conclusions

A numerical study of the occurrence of mechanical equilibrium instability and subsequent structure formation in the  $\text{He} + \text{CO}_2 - \text{N}_2$  gas system at different carbon dioxide content in the mixture can be carried out on the basis of the method of lattice Boltzmann equations. For the system under consideration, despite the implementation in the initial stage of mixing of the conditions for the mixture density to decrease with height, diffusion and convective types of mixing are recorded. The presented mathematical model makes it possible to describe the process of formation of a convective structure for various compositions of the ternary mixture. The obtained isoconcentration distributions in a vertical flat channel are discussed in detail and make it possible to specify the types of mixing and explain the occurrence of convection for the situation when, at the initial moment of time, the density of the gas mixture in the upper part of the diffusion channel is less than in the lower part. The main conclusions of this study are as follows:

1. The occurrence of convective instability can be associated with a significant curvature of isoconcentration distributions, which are absent during diffusion. The concentration profiles obtained are not typical for diffusion.
2. The disappearance of curvature in isoconcentration lines occurs at a certain initial composition of the mixture. For these calculation conditions, this occurs when the content of carbon dioxide is less than 0.3 mole fractions and determines the diffusion mode of mixing.
3. The degree of curvature of the concentration distributions depends on the content of the component with the highest molecular weight in the system. An increase in the concentration of the component with the highest molecular weight leads to a rise in the characteristic mixing times.
4. Further evolution of multicomponent mixing can result in the creation of convective formations and a “drop” flow regime.
5. The given distributions of pressure and average kinetic energy show the complex structure of the resulting flow. The maximum values of the distribution of pressure and kinetic energy correspond to the formation of convective structures.

**Author Contributions:** Conceptualization, V.K. and O.F.; methodology, V.K. and O.F.; software, D.Z. and A.Z.; validation, V.K. and D.Z.; formal analysis, O.F.; investigation, A.Z.; resources, D.Z.; data curation, A.Z.; writing—original draft preparation, V.K. and O.F.; writing—review and editing, V.K. and O.F.; visualization, A.Z.; supervision, V.K. and O.F.; project administration, V.K.; funding acquisition, V.K. All authors have read and agreed to the published version of the manuscript.

**Funding:** The Committee of Science of the Ministry of Science and Higher Education of the Republic of Kazakhstan supported this work (the project number: AP14870237).

**Institutional Review Board Statement:** Not applicable.

**Informed Consent Statement:** Not applicable.

**Data Availability Statement:** Data are contained within the article.

**Conflicts of Interest:** The authors declare no conflicts of interest.

## Abbreviations

### Symbols

$A_i$	[-]	dimensionless initial concentration gradient of the i-th component
$C$	[-]	component concentration
$c_i$	[-]	concentration of the i-th component
$D_{ij}^*$	[m <sup>2</sup> /s]	diffusion complexes
$F_i$	[-]	external force component
$H$	[m]	height
$Pr$	[-]	Prandtl number
$Ra$	[-]	Rayleigh number
$T$	[K]	temperature
$\vec{e}_i$	[-]	discrete velocities
$f_i$	[-]	velocity distribution function
$g$	[m/s <sup>2</sup> ]	free-fall acceleration scalar
$h_i$	[-]	concentration distribution function
$p$	[Pa]	pressure
$r$	[m]	radius
$t$	[s]	time
$\vec{u}$	[m/s]	weight-average velocity vector
$\vec{v}$	[m/s]	number-average velocity vector
$x$	[-]	abscissa axis
$\beta_i$	[-]	concentration analogue of the thermal expansion coefficient
$\nu$	[m <sup>2</sup> /s]	kinetic viscosity
$\rho$	[kg/m <sup>3</sup> ]	density
$\tau$	[-]	mesh relaxation time
$\omega_i$	[-]	weight coefficient depending on the number of discrete velocity

### Subscripts and Superscripts

$i, j, \alpha$	numbering of components
eq	equilibrium value
lbm	lattice Boltzmann equations method
phy	physical
/	notion of the perturbed quantity

## References

1. Raju, K.S. *Fluid Mechanics, Heat Transfer, and Mass Transfer: Chemical Engineering Practice*; John Wiley & Sons, Inc.: Hoboken, NJ, USA, 2011.
2. Carta, G. *Heat and Mass Transfer for Chemical Engineers: Principles and Applications*; McGraw-Hill Education: New York, NY, USA, 2021.
3. Ryzhkov, I.I.; Shevtsova, V.M. On thermal diffusion and convection in multicomponent mixtures with application to the thermogravitational column. *Phys. Fluids* **2007**, *19*, 027101. [[CrossRef](#)]
4. Gershuni, G.Z.; Zhukhovitskii, E.M. *Convective Stability of Incompressible Fluids*; Keter: Jerusalem, Israel, 1976.
5. Nield, D.A.; Bejan, A. *Convection in Porous Media*; Springer: New York, NY, USA, 2006.
6. Xie, C.; Tao, J.; Li, J. Viscous Rayleigh-Taylor instability with and without diffusion effect. *Appl. Math. Mech.—Engl. Ed.* **2017**, *38*, 263–270. [[CrossRef](#)]
7. Vadasz, P. Instability and Convection in Rotating Porous Media: A Review. *Fluids* **2019**, *4*, 147. [[CrossRef](#)]
8. Carballido-Landeira, J.; Trevelyan, P.M.J.; Almarcha, C.; De Wit, A. Mixed-mode instability of a miscible interface due to coupling between Rayleigh-Taylor and double-diffusive convective modes. *Phys. Fluids* **2013**, *25*, 024107. [[CrossRef](#)]
9. Bakhuis, D.; Ostilla-Mónico, R.; van der Poel, E.P.; Verzicco, R.; Lohse, D. Mixed insulating and conducting thermal boundary conditions in Rayleigh-Bénard convection. *J. Fluid Mech.* **2018**, *835*, 491–511. [[CrossRef](#)]
10. Radko, T.A. *Double-Diffusive Convection*; Cambridge University Press: Cambridge, UK, 2013.
11. Backhaus, S.; Turitsyn, K.; Ecke, R.E. Convective instability and mass transport of diffusion layers in a Hele-Shaw geometry. *Phys. Rev. Lett.* **2011**, *106*, 104501. [[CrossRef](#)] [[PubMed](#)]
12. Shevtsova, V.; Santos, C.; Sechenyh, V.; Legros, J.C.; Mialdun, A. Diffusion and Soret in Ternary Mixtures. Preparation of the DCMIX<sub>2</sub> Experiment on the ISS. *Microgravity Sci. Technol.* **2014**, *25*, 275–283. [[CrossRef](#)]
13. Matsuura, H.; Nagasaka, Y. Soret forced Rayleigh scattering instrument for simultaneous detection of two-wavelength signals to measure Soret coefficient and thermodiffusion coefficient in ternary mixtures. *Rev. Sci. Instrum.* **2018**, *89*, 024903. [[CrossRef](#)]

14. Lyubimova, T.P.; Zubova, N.A. Onset and nonlinear regimes of the ternary mixture convection in a square cavity. *Eur. Phys. J. E* **2015**, *38*, 19. [[CrossRef](#)]
15. Larabi, M.A.; Mutschler, D.; Mojtabi, A. Thermal gravitational separation of ternary mixture n-dodecane/isobutylbenzene/tetralin components in a porous medium. *J. Chem. Phys.* **2016**, *144*, 244902. [[CrossRef](#)]
16. Budroni, M.A.; Lemaigre, L.; De Witb, A.; Rossi, F. Cross-diffusion-induced convective patterns in microemulsion systems. *Phys. Chem. Chem. Phys.* **2015**, *17*, 1593–1600. [[CrossRef](#)]
17. Dil'man, V.V.; Lipatov, D.A.; Lotkhov, V.A.; Kaminskii, V.A. Instability in Unsteady-state Evaporation of Binary Solutions into an Inert Gas. *Theor. Found. Chem. Eng.* **2005**, *39*, 566–572. [[CrossRef](#)]
18. Kosov, V.N.; Fedorenko, O.V.; Asembaeva, M.K.; Mukamedenkyzy, V. Changing Diffusion–Convection Modes in Ternary Mixtures with a Diluent Gas Changing Diffusion–Convection Modes in Ternary Mixtures with a Diluent Gas. *Theor. Found. Chem. Eng.* **2020**, *54*, 289–296. [[CrossRef](#)]
19. Kaminskii, V.A.; Obvintseva, N.Y. Evaporation of a liquid under the conditions of convective instability in the gas phase. *Russ. J. Phys. Chem. A* **2008**, *82*, 1215–1220. [[CrossRef](#)]
20. Dil'man, V.V.; Lotkhov, V.A. Molecular turbulent evaporation in a gravitational field. *Theor. Found. Chem. Eng.* **2015**, *49*, 102–106. [[CrossRef](#)]
21. Moldabekova, M.S.; Asembaeva, M.K.; Akzholova, A.A. Experimental investigation of the instability of the mechanical equilibrium of a four-component mixture with ballast gases. *J. Eng. Phys. Thermophys.* **2016**, *89*, 417–421. [[CrossRef](#)]
22. Kossov, V.; Fedorenko, O.; Asembaeva, M.; Mukamedenkyzy, V.; Moldabekova, M. Intensification of the Separation of Isothermal Ternary Gas Mixtures Containing Carbon Dioxide. *Chem. Eng. Technol.* **2021**, *44*, 2034–2040. [[CrossRef](#)]
23. Kossov, V.; Fedorenko, O.; Kalimov, A.; Zhussanbayeva, A. Diffusion mechanisms for the occurrence of the instability of mechanical equilibrium of a ternary gas mixture containing carbon dioxide. *Fluids* **2021**, *6*, 177. [[CrossRef](#)]
24. Succi, S. *The Lattice Boltzmann Equation for Fluid Dynamics and Beyond*; Oxford University Press: Oxford, UK, 2001.
25. Huang, H.; Sukop, M.C.; Lu, X. *Multiphase Lattice Boltzmann Methods: Theory and Application*; Wiley-Blackwell: Hoboken, NJ, USA, 2015.
26. Feng, X.; He, Y.; Liu, D. Convergence analysis of an implicit fractional-step method for the incompressible Navier–Stokes equations. *Appl. Math. Modell.* **2011**, *35*, 5856–5871. [[CrossRef](#)]
27. Kossov, V.; Fedorenko, O.; Zhakebayev, D.; Mukamedenkyzy, V.; Kulzhanov, D. Convective mass transfer of a binary gas mixture in an inclined channel. *Z. Angew. Math. Mech.* **2022**, *102*, e201900197. [[CrossRef](#)]
28. Landl, M.; Prieler, R.; Monaco, E.; Hochenauer, C. Numerical investigation of conjugate heat transfer and numerical convection using the Lattice-Boltzmann method for realistic thermophysical properties. *Fluids* **2023**, *8*, 144. [[CrossRef](#)]
29. Navon, I.M. Pent: A periodic pentodiagonal systems solver. *Commun. Appl. Numer. Methods* **1987**, *3*, 63–69. [[CrossRef](#)]
30. Kim, J.; Moin, P. Application of a fractional-step method to incompressible Navier-Stokes equations. *J. Comput. Phys.* **1985**, *59*, 308–323. [[CrossRef](#)]
31. Zhumali, A.S.; Satenova, B.A.; Karuna, O.L. Lattice Boltzmann method simulation of thermal flow dynamics in a channel. *Int. J. Math. Phys.* **2019**, *10*, 75–81. [[CrossRef](#)]
32. Krüger, T.; Kusumaatmaja, H.; Kuzmin, A.; Shardt, O.; Silva, G.; Viggen, E.M. *The Lattice Boltzmann Method*; Springer International Publishing: Cham, Switzerland, 2017.
33. Guo, Z.; Zheng, C.; Shi, B. Discrete lattice effects on the forcing term in the lattice Boltzmann method. *Phys. Rev. E* **2002**, *65*, 046308. [[CrossRef](#)] [[PubMed](#)]
34. Seta, T. Implicit temperature-correction-based immersed-boundary thermal lattice Boltzmann method for the simulation of natural convection. *Phys. Rev. E* **2013**, *87*, 063304. [[CrossRef](#)]
35. Vargaftik, N.B. *Handbook of Physical Properties of Liquids and Gases. Pure Substances and Mixtures*; Springer: Berlin/Heidelberg, Germany, 2014.
36. Poling, B.E.; Prausnitz, J.M.; O'Connell, J.P. *The Properties of Gases and Liquids*; Mc-Graw-Hill Education: New York, NY, USA, 2000.

**Disclaimer/Publisher's Note:** The statements, opinions and data contained in all publications are solely those of the individual author(s) and contributor(s) and not of MDPI and/or the editor(s). MDPI and/or the editor(s) disclaim responsibility for any injury to people or property resulting from any ideas, methods, instructions or products referred to in the content.